

Competing orders suppressed by disorder around a hidden quantum critical point in cuprate high T_c superconductors.

S. Sanna,^{1,*} F. Coneri,² A. Rigoldi,³ G. Concas,³ S. Giblin,⁴ and R. De Renzi²

¹*Dipartimento di Fisica A. Volta, Università di Pavia, Via Bassi, 6, I-27100 Pavia, Italy*

²*Dipartimento di Fisica, Università di Parma, Viale G.Usberti, 7A, I-43100 Parma, Italy*

³*Dipartimento di Fisica, Università di Cagliari, Italy*

⁴*ISIS Facility, STFC-Rutherford Appleton Lab, HSIC, Didcot, OX110QX, U. K.*

(Dated: May 18, 2022)

We report extensive muon spin rotation measurements on the lightly doped $Y_{1-x}Ca_xBa_2Cu_3O_{6+y}$ compound, which allows us to disentangle the effect of disorder, controlled by random Ca^{2+} substitution, from that of mere doping. A 3D phase diagram of lightly doped cuprates is accurately drawn, showing that a *thermally activated* antiferromagnetic phase competes with superconductivity around a quantum critical point, hidden underneath a *frozen* insulating magnetic state. Disorder suppresses both competing order parameters and unveils the underlying frozen state. Doping and disorder destroy the activated magnetic phase along a line of first order phase transitions that ends at the critical point.

It is well known that the high T_c superconductivity of cuprates occurs nearby the disruption of an antiferromagnetic (AF) phase. In the pure $YBa_2Cu_3O_{6+y}$ compound [1–5] for increasing hole doping the AF phase is directly followed by the onset of superconductivity (SC). The incipient superconductor coexists with low temperature magnetic order [4], also called cluster spin glass. In $Y_{1-x}Ca_xBa_2Cu_3O_6$, $La_{2-x}Sr_xCuO_4$ and $Ca_xLa_{1.25-x}Ba_{1.75-x}Cu_3O_{6+y}$ the latter becomes the sole order parameter in a wide doping range [6, 7] between the suppression of T_N and the onset of T_c . These systems are classified as dirty [8] since they contain disordered substitutional heterovalent cations, i.e. strong Coulomb impurities in the vicinity of the CuO_2 layers. In this respect pure $YBa_2Cu_3O_{6+y}$ approaches the clean limit.

The lightly doped AF phase of both clean and dirty cuprates is characterized by two regimes [6, 9, 10]: a low temperature re-entrant phase, where the Cu moments recover the full value of $0.6 \mu_B$ appropriate for a two dimensional Heisenberg quantum antiferromagnet, and a high temperature antiferromagnetic phase, where both the moment $m(h)$ and $T_N(h)$ are strongly reduced by the hole doping h . In a parallel work [11] we showed that in the clean limit the crossover between these two regimes is connected with the thermal activation of charge carriers, with a low activation temperature $T_A(h)$, displayed in Fig. 1b. T_N is actually the critical temperature of a *thermally activated* antiferromagnet (TAAF), characterized by a metallic behavior [12]. The magnetic ground states in the re-entrant region and, at higher doping, in the coexistence region are shown to be the same [11]. We dub this state a *frozen* antiferromagnet (FAF). In the clean compound (a bad metal [13] where the AF and the SC ground states compete) the curve describing $T_N(h)$ and $T_c(h)$ merge at $T = 0$ for $h_{c0} = 0.056(2)$. This coincidence suggests the presence of a quantum critical point (QCP), hidden underneath the FAF state.

Here we report an accurate investigation of the cuprate

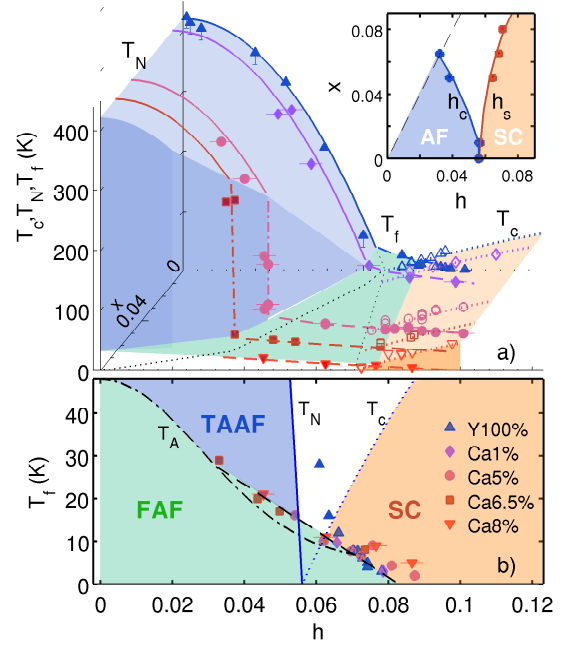


FIG. 1: (color on-line) Doping (h) and disorder (x , Ca content) dependence in $Y_{1-x}Ca_xBa_2Cu_3O_{6+y}$: a) Phase diagram; inset: critical hole densities $h_c(x)$ and $h_s(x)$, the dashed line is the $h = x/2$ lower limit; b) Zoom of $T_f(h, x)$, projected on the $x = 0$ plane; solid, dotted and dashed-dotted curves are the clean limit T_N , T_c , and T_A , respectively, from Ref. 11.

behavior under controlled disorder conditions. Our results show that the competing AF and SC orders are suppressed around the hidden QCP by Coulomb-driven disorder, which unveils the underlying intrinsic FAF state, that may coexist with superconductivity. We investigated the model system $Y_{1-x}Ca_xBa_2Cu_3O_{6+y}$ where the random Coulomb potential of Ca^{2+} impurities controls disorder, while hole doping is tuned by oxygen content.

Five series of polycrystalline samples are investigated, with $x = 0, 0.01, 0.05, 0.065, 0.08$ (henceforth Y100%, Ca1%, Ca5%, Ca6.5%, Ca8%), which are the same of Ref. [14].

Figure 1a shows a three dimensional view of the $Y_{1-x}Ca_xBa_2Cu_3O_{6+y}$ phase diagram, that summarizes our results. The magnetic transition temperatures, the Néel T_N and the low temperature order transition T_f , are obtained from Zero-Field μ SR, applying standard analysis described elsewhere [9, 11]. The superconducting transitions and the hole contents are from Ref. 14. These results disentangle the influence of doping, h , and disorder, x , showing that the portion of the green region where T_f is the only transition continuously widens with increasing Ca content, i.e. with disorder. A similar conclusion was qualitatively shown in earlier work on Zn substitution [3], across different cuprate families [6], and in irradiated samples [15].

Let us clarify the distinct influence of doping and disorder on Fig.1a. Dotted parabola describe the superconducting transitions $T_c(h)$, which shift rigidly to higher onsets $h_s(x)$ with Ca content, as previously reported [14]. Solid parabola represent the doping dependence of the Néel temperature $T_N(h) = T_{N0}(1 - (h/h_{c0})^2)$ in the clean limit, with $T_{N0} = 422(5)$ K and $h_{c0} = 0.056(2)$ [11]. Remarkably the same function, with no adjustable parameters, agrees with the low hole density data of Ca1% (diamonds) and Ca5% (circles), demonstrating that $T_N(h)$ is, at least initially, a universal function of doping, independent of the disorder parameter x . A first-order transition from high T_N values to much lower T_f values (dash-dotted lines in Fig. 1a) interrupts this behavior at Ca dependent critical hole densities, $h_c(x)$. A similar abrupt jump is displayed also by $Ca_xLa_{1.25}Ba_{1.75-x}Cu_3O_{6+y}$, a system where doping can be varied at fixed disorder [16]. The slightly asymmetric influence of disorder on the two critical hole densities, h_c and h_s , is plotted in the inset of Fig. 1a. As it is emphasized in the 3D view of the main panel, the convergence of the dotted lines describing h_c and h_s in the (h, x) plane and of T_N and T_c in the (T, h) plane strongly suggests the existence of a QCP at $h = 0.056$ in the clean limit. Notice that although $La_{2-x}Sr_xCuO_4$ experiments explore a portion of this diagram far from the QCP, its existence has been already suggested [17].

Another very interesting point is the doping and Ca dependence of the low transition temperature T_f (dashed curves in Fig. 1a). Figure 1b projects the $T_f(h, x)$ data on the (T, h) plane revealing that they all fall on the same dashed line, from $x = 0$ to $x \approx 0.08$. Notice that this line lies very close to the activation temperature $T_A(h)$ detected in the clean limit compounds [11] (solid curve), i.e. at the crossover between the FAF state and the thermally activated AF regime. Therefore disorder does not modify appreciably the border of the FAF phase, which is robust and hides the QCP also in pure Y100%. The

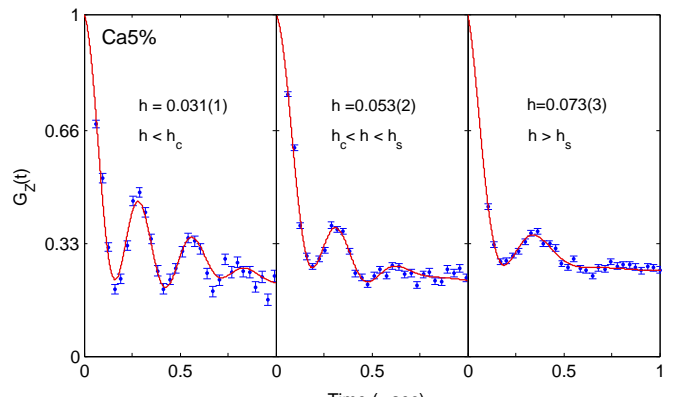


FIG. 2: (color on-line) Ca5% ($h_c = 0.04$, $h_s = 0.068$): muon asymmetry at $T = 2$ K with best fits for three very different hole densities.

linear trend is obeyed by all but a small number of points. The deviations regard pure Y100% at one end, for sample $h = 0.06$, where $T_N(h)$ is falling to zero from much higher values (e.g. $T_N = 60$ K at $h = 0.052$), and Ca doped samples at the opposite end, for large hole densities, where the FAF regime is slightly extended by disorder, in agreement with theoretical predictions [18].

Figure 2 shows the very similar time evolution of the zero field muon asymmetry at $T = 2$ K, in three Ca5% samples with different hole densities, respectively $h = 0.031 < h_c$ ($T_N = 258$ K), $h_c < h = 0.053 < h_s$ ($T_f = 16.1$ K) and $h = 0.073 > h_s$ ($T_f = 7.7$ K), within the green region of Fig. 1b. Solid curves are best fits to the standard ZF functions for polycrystals [11]. The oscillations are due to the muon spin precession around the magnetic field B_μ at the muon site [11, 19], which is proportional to the average local Cu moment. Apart from a modest frequency reduction, the main difference between the three samples is an increase of the damping, up to a maximum relative value $\Delta m/m = \Delta B_\mu/B_\mu = 0.3$, that indicates inhomogeneity, but still within a well ordered magnetic state, as it is demonstrated by the oscillatory pattern still present for $h > h_s$. In contrast muon precessions in typical spin glasses are strongly overdamped, due to a very broad distribution of local fields [20], with $\Delta B/B \gtrsim 1$ (i.e. width comparable to the mean value). We propose to abandon the spin glass terminology for cuprates, recognizing that earlier reports [21] identify an inhomogeneous, but not truly glassy magnetic state. This state is the same frozen antiferromagnet at very low doping, below T_A , and at higher doping, below T_f .

The line boundary of the FAF region in Fig. 1b marks the transition from an insulating to the bad metal state that displays a high temperature metallic behavior for all dopings (antiferromagnetic, paramagnetic as well as superconducting samples), as determined by transport [12, 22]. The common *bad-metal* character of these sam-

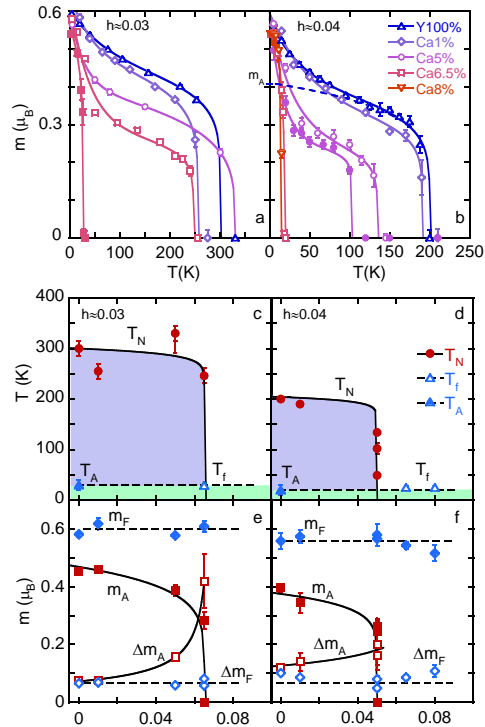


FIG. 3: (color on-line) Samples at constant hole densities: Temperature dependence of the magnetic moment with the best fit to Eq. 1, for the $h \approx 0.03$ (a) and $h \approx 0.04$ (b) samples. The dashed line shows an example of the low T extrapolation m_A ; c) and d) Ordering (T_N , T_f) and activation (T_A) temperatures; e) and f) Magnetic moment and width of its distribution in the FAF (m_F , Δm_F) and in the TAAF regime (m_A , Δm_A).

ples consists in a Fermi wave vector much less than the inverse mean free path, well below the Mott-Ioffe-Regel limit [22]. The FAF state, of course, remains properly insulating only to the left of h_s , while on the right nanoscopic coexistence with percolating SC precludes the assessment of the FAF clusters transport properties.

We now consider the disorder dependence of the staggered magnetic moment. The magnetic structure does not change with doping and the local muon field B_μ remains proportional [11] to the staggered Cu moment, that is measured as $m(h, T) = m_0 B_\mu(h, T)/B_{\mu 0}$, where $m_0 = 0.6 \mu_B$ and $B_{\mu 0}$ is the local field value in the unsubstituted parent compound at $T = 0$. Let us focus on two slices of the phase diagram of Fig. 1a, at constant doping versus disorder, for $h \approx 0.03$ and 0.04 . The temperature dependence of $m(T)$ is displayed in Fig. 3a, b for different values of x (disorder) in the slices. Best-fit solid curves follow a power-law behavior [11]

$$m(T) = [m_A + (m_F - m_A)e^{-cT}](1 - T/T_m)^\beta \quad (1)$$

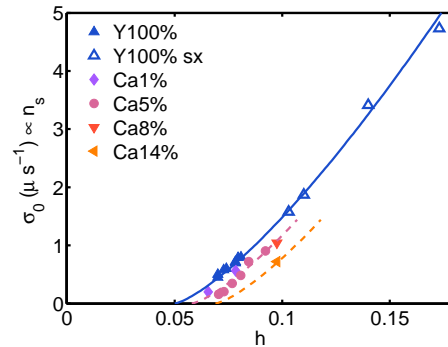


FIG. 4: (color on-line) Dependence on hole doping of the $T = 0$ μ SR relaxation rate $\sigma \propto n_s$ from TF- μ SR data: Y100%, filled triangle [4], Y100% sx, open triangle [23], Ca samples [14]. The solid curve is from fig. 8, Ref 23, rigidly shifted for the Ca substitution (dashed lines).

describing the low temperature upturn due to the smooth moment crossover between the FAF and the TAAF regimes. The parameter m_F is the $T \rightarrow 0$ value of the moment in the FAF state, whereas m_A is the low temperature extrapolation of the power law in the TAAF regime, as shown e.g by the dashed line in Fig. 3b.

The best fit parameters m_A and m_F are shown in Fig. 3, panels e, f, and the corresponding transition temperatures in panels c, d. Disorder suppresses T_N , and the TAAF phase with it, unveiling the underlying FAF phase which is unaltered ($T_A \approx T_f$). The first order nature of the transition between samples with and without a TAAF phase is apparent also when cut along the disorder axis (panels c and d). The moment m_F in the FAF state is constant vs. x (in each panel, e, f), and very weakly h -dependent (across the two panels), approaching the value $0.6 \mu_B$ of the clean undoped parent compound. It agrees with the magnetic-site dilution regime [11] appropriate for this truly insulating localized-moment state, as in clean $YBa_2Cu_3O_{6+y}$. A totally different conclusion applies to the TAAF regime, where the moment (m_A) is strongly dependent both on x and h , due to the peculiar topology of spin and mobile holes in the TAAF, as discussed in more details in Ref. 11. Disorder appears to enhance the suppression of the TAAF order, amplifying the disruptive effect of thermal activation. Accordingly, the behavior of the widths is respectively disorder dependent for Δm_A and independent for Δm_F .

Before concluding, we briefly recall that in the phase diagram to the right of the QCP disorder raises the threshold $h_s(x)$ for the onset of a superconducting condensate n_s . This quantity is proportional to the relaxation rate σ_0 measured in transverse field (TF) μ SR, and it is directly shown in Fig. 4, that summarizes our measurements in a field of 20 mT on the same samples investigated here [14]. The open symbols and the solid line represent the $YBa_2Cu_3O_{6+y}$ data and their interpolation

from Ref. 23, rescaled to polycrystalline values [24] and to low fields (fig. 6 of Ref. 23). The Y100% data fall on the same curve. For larger values of x the data and their dashed interpolation shift to the right, indicating that Coulomb disorder suppresses T_c and the superconducting order parameter n_s with it by reducing the hole density available for superconductivity.

This is a (nearly) symmetric effect to the suppression of T_N and of the related magnetic order parameter m_A on the left of the QCP, where the first order transition induced by disorder precipitates all cuprates (e.g. Fig. 3c, d) from the bad-metal TAAF regime into the underlying FAF insulating state, at a Ca dependent hole density $h_c(x)$. In this sector of the phase diagram the main effect of the increasing disorder appears to be a lowering of the threshold $h_c(x)$ for the suppression of TAAF magnetism. Disorder seems to be simply unveiling the intrinsic FAF behavior, by pushing aside the metallic AF and SC states from the hidden QCP. Notice that whereas disorder suppresses both order parameters it does not modify the metallic character of high temperature transport [12]. The boundary of the FAF phase in Fig. 1b is the same for all x values, at least up to $h = 0.075$, indicating that most of this phase is quite insensitive to disorder. This is an argument against a cluster spin glass introduced by disorder [8]. The unique $T_f(h)$ and the related $T_A(h)$ rather indicate an intrinsic origin, connected to the thermally activated crossover [11] in the self-organized charge and spin fabric (spin spirals [25] and/or stripes [26]) of the doped Mott-Hubbard system.

Summarizing, the behavior in the whole phase diagram agrees with the following simple notions, referred to Fig. 1b. Charge localization characterizes the green region of the phase diagram, where the insulating FAF magnetism is just diluted by doping and largely insensitive disorder. The remaining regions correspond to a bad metal state, where the TAAF and the SC compete around a QCP. The bad metal appears by thermal activation on the left of the QCP, but it is one of the two $T = 0$ ground state on the right, where SC sets in. The bad metal is very sensitive to charged impurity disorder, leading to the suppression of both its competing AF and SC order parameters, but not of its bad metal character. We finally notice that a line of first order transitions $h_c(x)$ terminates from the left in a second order QCP. The steeper $h_s(x)$ curve represents the onset of superconductivity in the regime of (nanoscopic) phase separation, hence a corresponding first order transition line may exist farther to the right. This simple description of the interplay between disorder and doping, with two first order lines terminating at the same QCP, awaits a full theoretical justification.

This work was carried out at the ISIS muon facility (RAL). We thank Lara Benfatto, José Lorenzana, Marco Grilli, Brian Andersen, Elbio Dagotto and Gonzalo Alvarez for stimulating discussions. Partial support

of PRIN-06 project and of the EU-NMI3 Access Programme is acknowledged.

* Samuele.Sanna@unipv.it

- [1] J. M. Tranquada, G. Shirane, B. Keimer, S. Shamoto, and M. Sato, *Physical Review B* **40**, 4503 (1989).
- [2] J. Rossat-Mignod, L. Regnault, M. Jurgens, C. Vettier, P. Burlet, J. Henry, and G. Lapertot, *Physica B* **163**, 4 (1990), ISSN 0921-4526.
- [3] H. Alloul, P. Mendels, H. Casalta, J. F. Marucco, and J. Arabski, *Physical Review Letters* **67**, 3140 (1991).
- [4] S. Sanna, G. Allodi, G. Concas, A. D. Hillier, and R. D. Renzi, *Phys. Rev. Lett.* **93**, 207001 (2004).
- [5] H. Alloul, J. Bobroff, M. Gabay, and P. J. Hirschfeld, *Reviews of Modern Physics* **81**, 45 (2009).
- [6] C. Niedermayer, C. Bernhard, T. Blasius, A. Gornik, A. Moodenbaugh, and J. I. Budnick, *Physical Review Letters* **80**, 3843 (1998).
- [7] A. Keren, A. Kanigel, and G. Bazalitsky, *Physical Review B (Condensed Matter and Materials Physics)* **74**, 172506 (2006).
- [8] E. Dagotto, *Science* **309**, 257 (2005).
- [9] S. Sanna, G. Allodi, and R. D. Renzi, *Solid State Communications* **126**, 85 (2003), ISSN 0038-1098.
- [10] F. C. Chou, F. Borsa, J. H. Cho, D. C. Johnston, A. Lascialfari, D. R. Torgeson, and J. Ziolo, *Physical Review Letters* **71**, 2323 (1993).
- [11] F. Coneri, S. Sanna, K. Zheng, J. Lord, and R. D. Renzi, arXiv:0911.5488.
- [12] Y. Ando, A. N. Lavrov, S. Komiya, K. Segawa, and X. F. Sun, *Physical Review Letters* **87**, 017001 (2001).
- [13] V. J. Emery and S. A. Kivelson, *Phys. Rev. Lett.* **74**, 32533256 (1995).
- [14] S. Sanna, F. Coneri, A. Rigoldi, G. Concas, and R. D. Renzi, *Phys. Rev. B* **77**, 224511 (2008).
- [15] F. Rullier-Albenque, H. Alloul, F. Balakirev, and C. Proust, *EPL* **81**, 37008 (2008).
- [16] R. Ofer, A. Keren, O. Chmaissem, and A. Amato, *Physical Review B (Condensed Matter and Materials Physics)* **78**, 140508 (2008).
- [17] C. Panagopoulos and V. Dobrosavljević, *Physical Review B* **72**, 014536 (2005).
- [18] B. M. Andersen and P. J. Hirschfeld, *Physical Review Letters* **100**, 257003 (2008).
- [19] M. Pinkpank, A. Amato, D. Andreica, F. Gyax, H. Ott, and A. Schenck, *Physica C* **317-318**, 299 (1999).
- [20] Y. J. Uemura, T. Yamazaki, D. R. Harshman, M. Senba, and E. J. Ansaldo, *Physical Review B* **31**, 546 (1985).
- [21] F. C. Chou *et al.*, *Phys. Rev. Lett.* **75**, 2204 (1995), A. N. Lavrov *et al.*, *Phys. Rev. Lett.* **87**, 017007 (2001), M. Matsuda *et al.*, *Phys. Rev. B* **65**, 134515 (2002), M-H. Julien, *Phys. B* **329-333**, 693 (2003), N. Hasselmann *et al.*, *Phys. Rev. B* **69**, 014424 (2004) C. Panagopoulos and V. Dobrosavljević, *Phys. Rev. B* **69**, 014536 (2005) I. Raičević *et al.*, *Phys. Rev. Lett.* **101**, 177004 (2008)
- [22] Y. Ando, *Journal of Physics and Chemistry of Solids* **69**, 3195 (2008), ISSN 0022-3697.
- [23] J. E. Sonier, S. A. Sabok-Sayr, F. D. Callaghan, C. V. Kaiser, V. Pacradouni, J. H. Brewer, S. L. Stubbs, W. N. Hardy, D. A. Bonn, R. Liang, et al., *Physical Review B*

- (Condensed Matter and Materials Physics) **76**, 134518 (2007).
- [24] W. Barford and J. Gunn, *Physica C* **156**, 515 (1988).
- [25] B. I. Shraiman and E. D. Siggia, *Physical Review Letters* **62**, 1564 (1989).
- [26] J. Zaanen and O. Gunnarsson, *Physical Review B* **40**, 7391 (1989).